J|A|C|S ARTICLES

Published on Web 07/02/2009

Porous Hollow Fe_3O_4 Nanoparticles for Targeted Delivery and Controlled Release of Cisplatin

Kai Cheng, Sheng Peng, Chenjie Xu, and Shouheng Sun*

Department of Chemistry, Brown University, Providence, Rhode Island 02912

Received April 30, 2009; E-mail: ssun@brown.edu

Abstract: We report a new approach to cisplatin storage and release using porous hollow nanoparticles (PHNPs) of Fe_3O_4. We prepared the PHNPs by controlled oxidation of Fe NPs at 250 °C followed by acid etching. The opening pores (~2−4 nm) facilitated the cisplatin diffusion into the cavity of the hollow structure. The porous shell was stable in neutral or basic physiological conditions, and cisplatin escape from the cavity through the same pores was a diffusion-controlled slow process with $t_{1/2} = 16$ h. However, in low pH (<6) conditions, the pores were subject to acidic etching, resulting in wider pore gaps and faster release of cisplatin with $t_{1/2} < 4$ h. Once coupled with Herceptin to the surface, the cisplatin-loaded hollow NPs could target to breast cancer SK-BR-3 cells with IC_{50} reaching 2.9 μM, much lower than 6.8 μM needed for free cisplatin. Our model experiments indicate that the low pH-responsive PHNPs of Fe_3O_4 can be exploited as a cisplatin delivery vehicle for target-specific therapeutic applications.

Introduction

Cisplatin (*cis*-diamminedichloro platinum(II)) has been widely used as a powerful therapeutic agent against numerous solid tumors by interacting with DNA to form intrastrand cross-link adducts and to interfere with cell transcription mechanism.[1] However, therapeutic applications of cisplatin have been restricted by its tendency in targeting both tumor and healthy cells, its chemical instability, its poor water solubility, and its low lipophilicity.[1−3] Furthermore, tumor cells may develop intrinsic resistances to cisplatin, which results in even less platin uptake and more DNA repair.[4] To alleviate these limitations and to increase the therapeutic efficacy, cisplatin is often coupled with hydrophilic polymers or embedded in liposomes or other types of polymeric micelles.[5−9] Such modifications have proven to be effective in enhancing cellular uptake and shielding reactive cisplatin from fast degradation *en route* to nuclear region. Various pH- or enzyme-dependent intracellular chemical stimuli have been applied to control the release and cellular distribution of cisplatin.[10,11] Recently, magnetic nanoparticles (NPs), especially biocompatible magnetite (Fe_3O_4) NPs, have been heavily pursued as versatile carriers for diagnostic and therapeutic applications. These NPs are superparamagnetic and are excellent contrast agents for magnetic resonance imaging (MRI).[12−21] Upon amphiphilic micelle or other bifunctional ligand coating, these NPs have been made with reduced nonspecific uptake by reticular-endothelial system (RES) and prolonged circulation in the physiological environments.[22−25] Drug molecules can be either attached to the NP surfaces via

(1) (a) Rosenberg, B.; Vancamp, L.; Krigas, T. *Nature* **1965**, *205*, 698. (b) Jung, Y. W.; Lippard, S. J. *Chem. Rev.* **2007**, *107*, 1387. (c) Wong, E; Giandomenico, C. M. *Chem. Rev.* **1999**, *99*, 2451. (d) Fuertes, M. A.; Alonso, C.; Perez, J. M. *Chem. Rev.* **2003**, *103*, 645.
(2) (a) Takahara, P. M.; Frederick, C. A.; Lippard, S. J. *J. Am. Chem. Soc.* **1997**, *119*, 4795. (b) Mantri, Y.; Lippard, S. J.; Baik, M. H. *J. Am. Chem. Soc.* **2007**, *129*, 5023.
(3) (a) Rajski, S. R.; Williams, R. M. *Chem. Rev.* **1998**, *98*, 2723. (b) Wang, D.; Lippard, S. J. *Nat. Rev. Drug Discovery* **2005**, *4*, 307.
(4) (a) Feazell, R. P.; Nakayama-Ratchford, N.; Dai, H.; Lippard, S. J. *J. Am. Chem. Soc.* **2007**, *129*, 8438. (b) Jamieson, E. R.; Lippard, S. J. *Chem. Rev.* **1999**, *99*, 2467. (c) Siddik, Z. H. *Oncogene* **2003**, *22*, 7265. (d) Reedijk, J. *Chem. Rev.* **1999**, *99*, 2499.
(5) Ramachandran, S.; Quist, A. P.; Kumar, S.; Lal, R. *Langmuir* **2006**, *22* (19), 8156.
(6) Xu, P.; VanKirk, E. A.; Murdoch, W. J.; Zhan, Y.; Isaak, D. D.; Radosz, M.; Shen, Y. *Biomacromolecules* **2006**, *7*, 829.
(7) Oishi, M.; Hayashi, H.; Michihiro, I. D.; Nagasaki, Y. *J. Mater. Chem.* **2007**, *17*, 3720.
(8) Ajima, K.; Murakami, T.; Mizoguchi, Y.; Tsuchida, K.; Ichihashi, T.; Iijima, S.; Yudasaka, M. *ACS Nano* **2008**, *2*, 2057.
(9) Matsumura, S.; Ajima, K.; Yudasaka, M.; Iijima, S.; Shiba, K. *Mol. Pharm.* **2007**, *4*, 723.
(10) Schmid, S. L.; Fuchs, R.; Male, P.; Mellman, I. *Cell* **1988**, *52*, 73.
(11) Schmid, S.; Fuchs, R.; Kielian, M.; Helenius, A.; Mellman, I. *J. Cell Biol.* **1989**, *108*, 1291.
(12) (a) Xu, C.; Sun, S. *Polym. Int.* **2007**, *56*, 821. (b) Gao, J.; Liang, G.; Zhang, B.; Kuang, Y.; Zhang, X.; Xu, B. *J. Am. Chem. Soc.* **2007**, *129* (5), 1428.
(13) Alivisatos, A. P. *Nat. Biotechnol.* **2004**, *22*, 47.
(14) Michalet, X.; Pinaud, F. F.; Bentolila, L. A.; Tsay, J. M.; Doose, S.; Li, J. J.; Sundaresan, G.; Wu, A. M.; Gambhir, S. S.; Weiss, S. *Science* **2005**, *307*, 538.
(15) Medintz, I. L.; Uyeda, H. T.; Goldman, E. R.; Mattoussi, H. *Nature* **2005**, *4*, 435.
(16) Wu, X.; Liu, H.; Liu, J.; Haley, K. N.; Treadway, J. A.; Larson, J. P.; Ge, N.; Peale, F.; Bruchez, M. P. *Nat. Biotechnol.* **2003**, *21*, 41.
(17) Jun, Y.-w.; Huh, Y.-M.; Choi, J.-S.; Lee, J.-H.; Song, H.-T.; KimKim; Yoon, S.; Kim, K.-S.; Shin, J.-S.; Suh, J.-S.; Cheon, J. *J. Am. Chem. Soc.* **2005**, *127*, 5732.
(18) Huh, Y.-M.; Jun, Y.-w.; Song, H.-T.; Kim, S.; Choi, J.-s.; Lee, J.-H.; Yoon, S.; Kim, K.-S.; Shin, J.-S.; Suh, J.-S.; Cheon, J. *J. Am. Chem. Soc.* **2005**, *127*, 12387.
(19) Song, H.-T.; Choi, J.-s.; Huh, Y.-M.; Kim, S.; Jun, Y.-w.; Suh, J.-S.; Cheon, J. *J. Am. Chem. Soc.* **2005**, *127*, 9992.
(20) Lee, J.-H.; Huh, Y.-M.; Jun, Y.-w.; Seo, J.-W.; Jang, J.-T.; Song, H.-T.; Kim, S.; cho, E.-J.; Yoon, H.-G.; Suh, J.-S.; Cheon, J. *Nat. Med.* **2007**, *13*, 95.
(21) Nasongkla, N.; Bey, E.; Ren, J.; Ai, H.; Khemtong, C.; Guthi, J. S.; Chin, S.-F.; Sherry, A. D.; Boothman, D. A.; Gao, J. *Nano Lett.* **2006**, *6*, 2427.
(22) Gupta, A. K.; Gupta, M. *Biomaterials* **2005**, *26*, 3995.
(23) Zhao, M.; Beauregard, D. A.; Loizou, L.; Davletov, B.; Brindle, K. M. *Nat. Med.* **2001**, *7*, 1241.

chemical modification or embedded in the double-layer coating around the NP surface. Despite these improvements, cisplatin and the derivative platin complexes still lack the desired target-specificity and therapeutic efficacy.

Here we report a new approach to cisplatin storage and release using porous hollow NPs (PHNPs) of Fe_3O_4. We recently succeeded in the synthesis of monodisperse hollow NPs (HNPs) of Fe_3O_4 via controlled oxidation of Fe NPs.[26] We noticed that the shell of these HNPs was polycrystalline and its crystallinity could be improved by prolonged heating in solution. With the crystal domain growing larger in the shell structure, the crystal boundaries in the polycrystalline structure opened up, resulting in the porous shell. Our further experiments indicated that the pore size could be controlled even more readily by acid etching, as Fe_3O_4 in the boundary area was more reactive and tended to be etched away first, leaving the open pores on the shell structure. We demonstrate that such PHNPs are ideal for cisplatin storage and targeted delivery. The open pores (~3 nm) (PHNPs-3) facilitate cisplatin diffusion into the cavity of the hollow structure. The porous shell is stable in neutral or basic physiological condition, and cisplatin escapes from the cavity through the same pores via a diffusion-controlled slow process. However, in low pH conditions, the pores are subject to acidic etching, resulting in wider pore opening and faster release of cisplatin. Once coupled with Herceptin, a humanized IgG1 monoclonal antibody,[27] the cisplatin-loaded hollow NPs can be targeted to breast cancer SK-BR-3 cells that overexpress human epidermal growth factor receptor 2 (HER2), not obviously to MDA-MB-231 cells that have less HER2 expression. Our model experiments show that the pH-responsive PHNPs can be exploited for target-specific therapeutic applications.

Experimental Section

Methods. ^1H and ^{13}C NMR spectra were recorded on a Bruker Hades 300 NMR spectrometer operating at 300 and 125 MHz, respectively. $CDCl_3$ was used as the solvent and served as an internal reference. Mass spectra of synthetic polymer linkers were measured using a time-of-flight (TOF) mass spectrometer (Voyager DE PRO) equipped with a matrix-assisted laser desorption ionization (MALDI) ion source. The fast atom bombardment ionization (FAB) for characterization of synthetic organic molecules was performed on a JEOL JMS-600H double focusing magnetic sector mass spectrometer. FTIR spectra were obtained on an ATI Mattson Infinity Series FTIR spectrophotometer. Compressed KBr pellets containing about 2 wt % of sample were used for these studies. Powder X-ray diffraction (XRD) experiments were performed on a Bruker AXS D8-Advanced diffractometer equipped with Cu Kα radiation ($\lambda = 1.5418$ Å). Fluorescence confocal scanning laser microscopy (CSLM) was performed using a Zeiss LSM510 Meta confocal laser-scanning microscope (CLSM). Graphical image analysis was performed using Adobe Photoshop. Three-dimensional reconstruction was accomplished using the Confocal Assistant or Zeiss LSM Image Browser. The TEM images were recorded with a Philips EM 420 instrument operating at 120 kV. Samples were dispersed on carbon films supported on copper grids. The energy disperse spectroscopy (EDS) was obtained using a LEO 1530-vp scanning electron microscope (SEM) equipped with the Oxford EDS system. The hydrodynamic diameters of various functionalized NPs were measured using a Malvern Zeta Sizer Nano S-90 dynamic light scattering (DLS) instrument. The hysteresis loop was recorded at 300 K with a LakeShore 7400 VSM system. UV−vis spectra between 200 and 850 nm were obtained using a PerkinElmer Lambda 35 UV−vis spectrometer. The element analysis of Fe and Pt in the samples was carried out by a JY2000 Ultrace inductively coupled plasma atomic emission spectrometer (ICP-AES) after aqua regia digest.

Materials. *N*-Hydroxysuccinimide (NHS) and 1-ethyl-3-(3-dimethylaminopropyl) carbodiimide hydrochloride (EDC) were purchased from Pierce Biotechnology. *O*,*O*′-Bis(2-aminopropyl) polypropylene glycol-*block*-poly(ethylene glycol)-*block*-poly(propylene glycol) (PEG-diamine, $M_r = 1{,}900$) was purchased from Sigma-Aldrich. Fluorescein 5(6) isothiocyanate (FITC) was obtained from Sigma-Aldrich. Triethylamine and dichloromethane (DCM) were distilled prior to use, and *N*,*N*′-dimethylformamide (DMF) was stored over molecular sieves. Other solvents and chemicals were used as received. Herceptin (Trastuzumab) was purchased from Genentech, Inc. All buffers and media were purchased from Invitrogen Corp. Deionized water was obtained from a Millipore Milli-DI Water Purification system. The dialysis membrane tubings (MWCO = 12,000−14,000 and 300,000) were purchased from Spectrum laboratories.

Synthesis of Heterobifunctional PEG Ligand. See Supporting Information.

Synthesis of 13 nm Fe/Fe_3O_4 NPs. A mixture solution of 1-octadecene (20 mL) and oleylamine (0.3 mL, 0.9 mmol) in a four-necked flask was degassed under argon at 120 °C for 30 min to remove the moisture and oxygen. As soon as the mixture solution was heated to 180 °C, 0.7 mL of iron pentacarbonyl ($Fe(CO)_5$) was quickly injected into the mixture with vigorous stirring under a blanket of argon. The mixture was kept at 180 °C for 30 min before being cooled to room temperature. After the supernatant was discarded, the magnetic stirring bar coated with black product was transferred into a centrifuge vial and then washed by hexanes in the presence of oleylamine under nitrogen protection, followed by adding 30 mL of isopropanol to precipitate the 13 nm Fe/Fe_3O_4 NP seeds. The washing step was repeated twice. The resultant NPs were redispersed in hexane in the presence of oleylamine (0.01 mL).

Synthesis of 16 nm HNPs of Fe_3O_4. A mixture solution of 1-octadecene (20 mL) and trimethyl amine *N*-oxide (30 mg) in a four-necked flask was degassed under argon at 130 °C for 1 h to remove the moisture and oxygen. Next, 80 mg of Fe/Fe_3O_4 NPs in hexane was quickly injected into the mixture, and the resultant mixture was kept at 130 °C for 2 h to remove hexane. The following procedures for controlled oxidation process were carried out at different temperatures with different heating times, i.e., the reaction mixture was maintained at 130 °C for 12 or 24 h before being cooled to room temperature. The additional heating steps were optional, i.e., the mixture was continuously heated to 210 °C at a heating rate of 2 °C/min for 2 h before being heated to 250 °C for 30 min, or the mixture was directly heated to 250 °C at a heating rate of 2 °C/min for 1 h. Once the resultant solution was cooled to room temperature, 40 mL of acetone was added into the mixture to precipitate the product, followed by centrifuging at 8500 rpm for 8 min. The black product was redispersed in hexane in the presence of oleylamine and then precipitated out by adding another 40 mL of acetone. After being collected by centrifugation, the resultant 16 nm HNPs were dispersed in hexane.

Synthesis of PHNPs of Fe_3O_4. A mixture solution of 0.17 mL (0.5 mmol) of oleylamine and 0.16 mL of oleic acid in 20 mL of benzyl ether in a four-necked flask was degassed with nitrogen at room temperature for 30 min. Next, 50 mg of HNPs of Fe_3O_4 in hexane was added into the above mixture via a syringe. The resulting mixture was heated to 100 °C with vigorous stirring and maintained at this temperature for 30 min to remove hexane. Subsequently, the solution was heated to 260 °C at a heating rate of 5 °C/min and kept at this temperature for 30 min before being cooled to room temperature. The different heating procedures were

(24) Laurent, S.; Forge, D.; Port, M.; Roch, A.; Robic, C.; Vander Elst, L.; Muller, R. N. *Chem. Rev.* **2008**, *108*, 2064.
(25) Jun, Y.-w.; Lee, J.-H.; Cheon, J. *Angew. Chem., Int. Ed.* **2008**, *47*, 5122.
(26) Peng, S.; Sun, S. H. *Angew. Chem., Int. Ed.* **2007**, *46*, 4155.
(27) Cuello, M.; Ettenberg, S. A.; Clark, A. S.; Keane, M. M.; Posner, R. H.; Nau, M. M.; Dennis, P. A.; Lipkowitz, S. *Cancer Res.* **2001**, *61*, 4892.

also studied. The black product was precipitated by adding 30 mL of acetone and then collected by centrifugation. The resultant PHNPs were washed three times by repetition of dispersion in hexane and precipitation with acetone and centrifugation.

Incorporation of Cisplatin in PHNPs of Fe_3O_4. Twenty milligrams of PHNPs of Fe_3O_4 were dispersed in 4 mL of a mixture of chloroform and DMF (2:1, v/v) containing 16 mg of cisplatin. Next, 80 mg of heterobifunctional PEG (DPA-PEG-COOH or DPA-PEG) in 2 mL of DMF was added dropwise over 6 h. The resultant mixture was stirred at room temperature for 24 h under nitrogen protection to allow penetration of cisplatin into the hollow interiors. DMF was evaporated under a nitrogen flow at room temperature. The remained solid at the bottom of the container was dispersed in a mixture of chloroform and DMF (4:1, v/v), followed by filtration to remove excess cisplatin. The cisplatin-containing PEGylated PHNPs (Pt-PHNPs) were precipitated by adding hexane and then collected by a permanent magnet. The resultant NPs in chloroform were filtered through a size-exclusion column (Lipophilic Sephadex) to separate unencapsulated cisplatin from NPs. The purified Pt-HPNPs were dispersed in water or PBS and then filtrated with 0.2 μm filter to eliminate any precipitation and microbial contamination. Finally, the Pt-PHNPs were either used immediately or lyophilized and stored in a freezer to prevent the unexpected leaking of cisplatin. The loading of cisplatin in the NPs was measured as the amount of Pt with ICP-AES analysis.

Kinetics of Cisplatin Release from Pt-PHNPs. The cisplatin release study was carried out in the dialysis membrane tubing (MWCO = 12,000). Pt-PHNPs cannot cross the membrane, but cisplatin can easily diffuse out. Once the lyophilized Pt-PHNPs were dispersed in water, they were immediately transferred into the dialysis membrane tubing. Typically, 1 mL of Pt-HPNP dispersion (1 mg Fe/mL, the concentrations of Fe and Pt were measured by ICP-AES) in dialysis membrane tubing was incubated at 37 °C in 40 mL of PBS buffer (137 mM NaCl, 10 mM phosphate, 2.7 mM KCl, pH = 7.4). A 1 mL aliquot was taken at predetermined time intervals over the period of 72 h and diluted up to 5 mL with 2% nitric acid for ICP-AES analysis. The total volume of PBS buffer was maintained by adding the same volume of fresh PBS buffer. The cumulative release profile of cisplatin from the Pt-HPNPs was obtained via the concentration correction (the amount of cisplatin in each aliquot was calculated to correct the overall cumulative releasing of cisplatin) of released cisplatin based on the following equation: $C_t' = C_t + (v/V)\sum_0^{t-1} C_t$, where C_t' is the corrected concentration at time t, C_t is the apparent concentration at time t, v is the volume of the aliquots taken, and V is the total volume of buffer. Three PBS buffers with different pH values (pH = 5.0, 6.0, and 7.4; the pH of PBS was adjusted using 1 M of HCl or 1 M NaOH) were prepared and used as incubation buffer for kinetic studies of cisplatin release as well.

Synthesis of FITC-Labeled PHNPs. Twenty milligrams of PHNPs were dispersed in 4 mL of chloroform containing 80 mg of heterobifunctional PEG (DPA-PEG-NH_2). The resultant mixture was stirred at room temperature for 24 h under nitrogen protection. The PEGylated NPs were precipitated by adding hexane, then collected by a permanent magnet, and dried under nitrogen. The resulting NPs were then dispersed in water or PBS. The unbound PEG linkers were removed by dialysis using a dialysis bag (MWCO = 12,000−14,000) for 24 h in water. The purified NPs were then filtrated through a 0.2 μm filter to eliminate any precipitation and microbial contamination.

Next, 3.58 μmol of the above PEGylated NPs (200 μg of Fe, based on the iron concentration determined by ICP-AES analysis) was dispersed in 1 mL of 50 mM sodium carbonate buffer (Na_2CO_3/$NaHCO_3$, pH = 9.3) before 10 μL of FITC (10 mg/mL in DMSO, 0.2568 μmol) was added. The reaction mixture was shaken for 1 h at room temperature. The unbound FITC was removed by a size-exclusion column (Sephadex G-25, PD-10 column, GE) from FITC labeled NPs. The purified NPs were then filtrated through a 0.2 μm filter to eliminate any precipitation and microbial contamination.

FITC-Labeled Herceptin or Rhodamine-Labeled Herceptin. Before labeling Herceptin with fluorescein, the pH of 200 μL of 10 mg/mL Herceptin solution was set to 9.3 via dialysis against 50 mL of 50 mM sodium carbonate buffer (pH = 9.3) at 4 °C for 24 h. The dialyzed Herceptin was diluted to a final concentration of 2 mg/mL with sodium carbonate buffer and then mixed thoroughly by vortexing after addition of 10 μL of 10 mg/mL FITC (0.2568 μmol) in DMSO. The reaction mixture in a vial was wrapped with aluminum foil and incubated at room temperature for 1 h. The unreacted FITC was removed by a size-exclusion column (Sephadex G25, PD-10, GE). The FITC labeled Herceptin was used immediately or stored in PBS buffer at 4 °C before use. Similarly, Herceptin was labeled with Rhodamine isothiocynate using the procedure described above.

Immobilization of Herceptin on PHNPs or Pt-PHNPs. A 8.95 μmol portion of PEGylated PHNPs (500 μg of Fe, based on the iron concentration determined by ICP-AES analysis) was dispersed in 0.5 mL of DI water. The estimation of the number of PHNPs was based on an assumption that the inner and outer diameters of monodisperse HNPs are 10 and 16 nm, respectively. The amount of attached PEG linkers on the HNPs was determined by TGA/DTG (ratio of PEG to particle is close to 40:1). The amount of EDC (0.75 mg, 3.92 μmol) added into the mixture was equivalent to 1000 times the amount of carboxylic acid on the particles. After 30 min of incubation, excess EDC molecules were removed by a size-exclusion column (Sephadex G25, PD-10, GE). Next, 500 μg of Herceptin (3.44 nmol) in 0.5 mL of PBS was added into the mixture. The resultant mixture was incubated at room temperature for 1 h. The uncoupled Herceptin was removed by dialysis using a dialysis bag (MWCO = 300,000) for 24 h in PBS. The purified Herceptin-bound PHNPs (Her-PHNPs) were stored in PBS at 4 °C before use. The similar procedure was used for immobilizing Herceptin on Pt-PHNPs, except for the purification step. In order to reduce the unavoidable cisplatin leakage, the as-synthesized Herceptin-PHNPs were filtered through a MWCO-300K NanoSep filter (FisherSci, Inc.) by centrifugation at 2500*g* for 3 min at 4 °C. The purified Her-Pt-PHNPs were either used immediately or lyophilized first and then stored at −20 °C.

Cell Lines and Cell Culture. The Her-2/Neu positive human mammary carcinoma cell line SK-BR-3 purchased from American Type Culture Collection (ATCC, Manassas, VA) were grown in Dulbecco's modified Eagle's medium (DMEM) medium supplemented with 10% fetal bovine serum (FBS) and 1% penicillin/streptomycin (Gibco BRL, Grand Island, NY) at 37 °C in a humidified 5% CO_2 atmosphere. The human mammary cell line MDA-MB-231, which is Her-2/Neu negative, was grown in same medium and condition.

Cellular Uptake of Her-PHNPs or Her-Pt-PHNPs. SK-BR-3 and MDA-MB-231 cell lines were cultured in DMEM with 10% FBS and 1% penicillin/streptomycin in T25 flasks. Cells were grown to near confluence, the medium was removed, and the cells were then washed twice with PBS. Cells were then exposed to Her-PHNPs/Her-Pt-NPs at a concentration of 10, 20, and 50 μg/mL in growth medium for 4 or 10 h. Control flasks received medium either without the particles or with unmodified PHNPs/Pt-HPNPs at different concentrations. After 4 or 10 h of incubation, the cells were washed twice with PBS and then detached using trypsin-EDTA. Trypsinized cells were collected by centrifugation at 1000 rpm for 5 min and resuspended in PBS. Cell counting was carried out using a hemacytometer. After centrifuge and removal of the supernatant, the cell pellets were lysed by aqua regia. The iron and platinum concentration were determined by ICP-AES. The assay was performed in triplicate.

Cytotoxicity of Pt-PHNPs and Her-Pt-PHNPs. Cell viability was determined in SK-BR-3 and MDA-MB-231 cells. Cytotoxicities of cisplatin, porous hollow NPs, Pt-PHNPs, and Her-Pt-PHNPs were evaluated using the MTT assay. Basically, cells were plated at a density of 1×10^4 in 96-well plates 24 h prior to the exposure to the above materials. Cells were incubated in the growth medium

containing different concentrations of cisplatin or Pt-PHNPs with same amount of cisplatin for 24, 48, or 72 h. After treatment, 3-(4,5-dimethylthiazol-2-yl)-2,5-diphenyltetrazolium bromide (MTT, 5 mg/mL in PBS) was diluted 1:100 with medium into each well. After 4 h of incubation, culture supernatants were aspirated, and purple insoluble MTT product was redissolved in 100 μL of DMSO in 10 min. The concentration of the reduced MTT in each well was determined spectrophotometrically by subtraction of the absorbance reading at 630 nm from that measured at 570 nm using a microplate reader. Cell viabilities were presented as the percentage of the absorbance of cisplatin-treated cells to the absorbance of nontreated cells and plotted as cisplatin concentration.

Immunofluorescence Staining. SK-BR-3 and MDA-MB-231 cells were plated onto coverslips (Corning, Corning, NY) in 12-well plates, respectively. Cell monolayers grown on glass coverslips were allowed to 70−80% confluence and then placed on ice. After the medium was aspirated, the cells were washed twice with PBS and fixed with 4% paraformaldehyde in PBS for 10 min at room temperature. The fixed cells were washed with PBS and then permeabilized in 0.1% Triton X-100/PBS for 10 min at room temperature. After incubation in PBS containing 1% bovine serum albumin (BSA) for 1 h at room temperature to block nonspecific binding, cells were incubated with Herceptin (20 μg/mL in PBS containing 0.1% BSA) for 1 h at room temperature, and then washed 3 times for 5 min in PBS containing 0.1% BSA. The cells were then incubated with an Alexa Fluor 488-conjugated secondary antibody (goat antihuman IgG, Sigma) diluted 1:200 in PBS containing 0.1% BSA for 1 h at room temperature. After washing with PBS, 4′,6-diamidino-2-phenylindole (DAPI) was used as a nuclear counterstain. The cells were then washed twice, and the coverslips were removed from the wells and mounted onto slides using Aqua Poly/Mount (Polysciences Inc.), and visualized by confocal scanning laser microscopy (CSLM). Controls consisted of cells stained in the absence of primary antibody. Surface-bound Herceptin is internalized by SK-BR-3 cells in a time-dependent manner. To examine kinetics of Herceptin uptake, SK-BR-3 cells were incubated with 20 μg/mL Herceptin labeled by a fluorescent dye (Rhodamine) for various intervals (1, 2, 4 or 6 h). Cells were then fixed and processed for dual-label CSLM.

Transfection and Internalization (Colocalization of Her-Pt-HPNPs and Endosomes). SK-BR-3 and MDA-MB-231 cells were plated onto coverslips in 12-well plates as previously described. Cell monolayers grown on glass coverslips were allowed to near 90% confluence and transfected with Rab5-DsRed WT (kindly provided by Dr. Maureen A. Chung, Rhode Island Hospital, Department of Surgery of Brown University, Addgene plasmid 13050) using Lipofectamine 2000 (Invitrogen), according to the manufacturer's instructions. Briefly, for each well, 3 μL of Lipofectamine 2000 diluted into 100 μL of OptiMEM medium was combined with 1 μg of Rab5 plasmid in 100 μL of OptiMEM medium, and the mixture was then incubated for 30 min at room temperature to allow the plasmid-Lipofectamine complexes to form. Meantime, cells were incubated for 30 min with OptiMEM before addition of the plasmid-Lipofectamine complexes in the absence of serum. The serum-free medium was changed with the growth medium after 4 h incubation. FITC-Her-PHNPs (10 μg/mL in growth medium) were added into the cell culture 10 h after transfection. Control received medium either without the particles or with FITC labeled PHNPs at same concentrations. After 10 h of incubation, cells were then fixed and processed for dual-label immunofluorescence CSLM as previously described.

TEM. SK-BR-3 and MDA-MB-231 cell lines were cultured in DMEM with 10% FBS and 1% penicillin/streptomycin in T75 flasks. Cells were grown to near confluence and then exposed to Her-PHNPs/Pt-PHNPs at the concentration of 50 μg Fe/mL in growth medium for 4 or 10 h. Control flasks received medium either without the particles or with unmodified PHNPs/Pt-PHNPs at same concentration. After incubation, the medium was removed, and the cells were then washed twice with PBS. Cells were fixed in 2.5% glutaraldehyde in 100 mM sodium cacodylate buffer (SCB, pH = 7.4) for 1 h at room temperature. The fixative solution was then removed and replaced with 1% BSA in SCB. The cells were gently harvested from the cell culture flask using a cell scraper and then collected by centrifugation at 5000 rpm for 5 min. The resulting cell pellets were washed 3 × 15 min with SCB containing 0.1 M glucose (pH = 7.4). The cell pellets were fixed in a freshly prepared mixture consisting of 1% osmium tetroxide in SCB for 1 h at room temperature. The resultant pellets were washed with SCB for 5−10 min, followed by two washings with water (5−10 min). After the secondary fixation and washing, the cell pellets were dehydrated using a graded series of ethanol according to the following schedule: 35% ethanol for 20 min, 50% ethanol for 20 min, 70% ethanol for 20 min, 100% ethanol for 3 × 20 min. The epoxy resin (10 g of ERL 4221 (cycloaliphatic epoxide resin ERL 4221), 25 g of NSA (nonenyl succinic anhydride), 8 g of DER-736 epoxy resin (polyglycol dieposides product), 0.3 g of DMAE (2-(dimethylamino) ethanol), Electron Microscopy Sciences) was introduced gradually into the cell pellets after dehydration. The pellets were embed in fresh resin and placed in an oven at 70 °C for 11 h. The polymerized blocks were allowed to cool at room temperature before sectioning. Semithin sections (1 μm) were cut with glass knives on a Reichert Ultracut microtome, stained with methylene blue−azure II, and evaluated for areas of cells. Ultrathin sections (90 nm) were cut with a diamond knife, retrieved onto 150 mesh copper grids, and examined with a Philips 410 TEM equipped with an Advantage HR CCD camera operating at 80 kV.

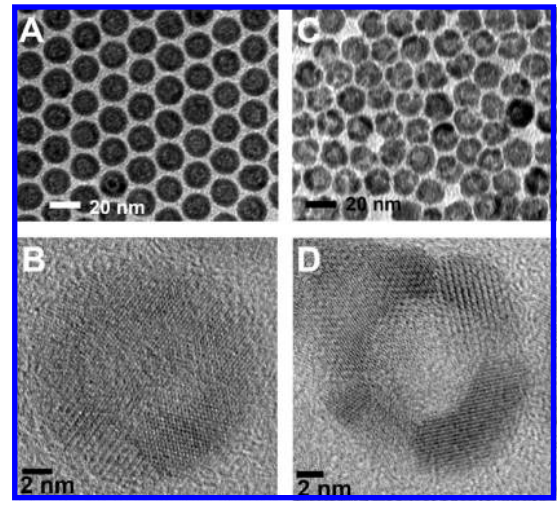

Figure 1. (A) TEM image of the 16 nm HNPs of Fe_3O_4. (B) HRTEM image of a single HNP. (C) TEM image of the 16 nm PHNPs of Fe_3O_4, (D) HRTEM image of a single PHNP.

Results and Discussion

Synthesis of Porous Hollow NPs (PHNPs) of Fe_3O_4. The monodisperse HNPs of Fe_3O_4 with an average diameter of 16 nm were prepared by controlled oxidation of amorphous core/shell Fe NPs in the presence of the oxygen-transfer reagent trimethylamine *N*-oxide (Me_3NO). The resultant HNPs have a Fe_3O_4 shell with a thickness of about 3 nm and a hollow interior about 10 nm in diameter as shown in Figure 1A. The shell consists of polycrystalline Fe_3O_4 as confirmed by XRD (Figure S1, Supporting Information) and high-resolution TEM (HR-TEM) (Figure 1B). The small Fe_3O_4 grains in the shell tend to grow into larger crystallites after treated at the high temperature (i.e., 260 °C), leading to the wider gap between two Fe_3O_4 crystal domains and the formation of pores in the shell (Figure 1C). The HRTEM image of the PHNPs shows that the spherical interior cavities are surrounded by discrete polycrystalline Fe_3O_4

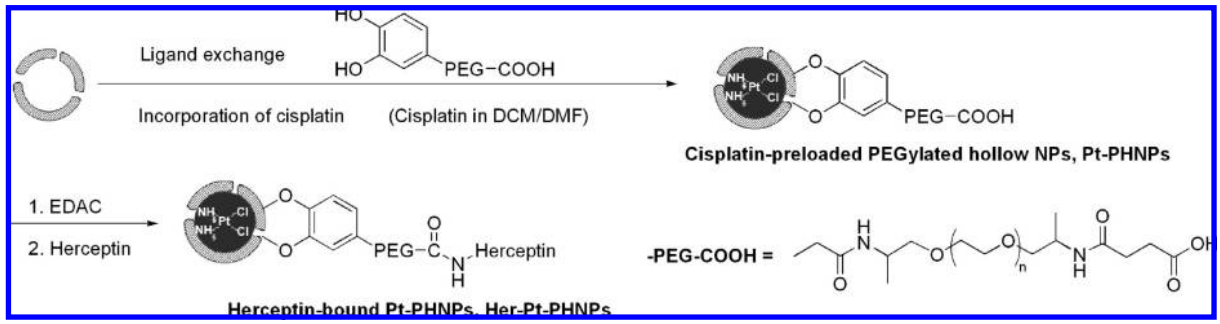

Figure 2. Schematic illustration of simultaneous surfactant exchange and cisplatin loading into a PHNP and functionalization of this PHNP with Herceptin.

domains. The gaps between discrete crystalline domains are around 2−4 nm (Figure 1D) and can be controlled by the temperature, heating time of the post thermal treatment as well as the amount of oleic acid and oleylamine used in the synthesis (see Supporting Information). Longer heating time results in larger pores on the shell structure with the resultant particles being in more faceted morphology due likely to the formation of the larger crystalline domains (Figure S2, Supporting Information).

Fe_3O_4 Surface Functionalization and Cisplatin Loading. The as-prepared PHNPs are coated with a layer of oleate/oleylamine and are hydrophobic. To make them hydrophilic and to provide an active functional group, we replaced the oleate/oleylamine coating with a catechol group from dopamine (DPA) that has been linked with PEG.[28] In this process, bifunctional PEG linkers were prepared as reported previously (see Supporting Information).[28] For the comparison, a monofunctional PEG linker methyl-PEG-OH was also prepared by a modified procedure.[28] TEM image analysis on the PEGylated NPs shows that there is no obvious change in the particle morphology and porous structures in the shell after the PEGylation with DPA-PEG-COOH. The hydrodynamic diameter of PEGylated NPs as measured by DLS is about 60 nm, indicative of the successful conjugation with DPA-PEG-COOH (Figure S3, Supporting Information). The PEGylated NPs are easily dispersed in the aqueous solution and show excellent stability in the physiological condition for more than 30 h (10% FBS in PBS at 37 °C) without any detectable agglomeration (Figure S4, Supporting Information). FTIR spectra further verify the successful functionalization of NPs with DPA-PEG-COOH (Figure S5, Supporting Information).

Cisplatin was loaded into PHNPs by the nanoprecipitation method.[8,9,29] Cisplatin is poorly soluble in water (2.53 mg/mL) and chloroform (<1 mg/mL) but better dissolved in DMF (20.0 mg/mL). To load cisplatin, the PHNPs-3 (PHNPs-*n*, *n* = average pore size in nanometer; see also Figure S2, Supporting Information) were dispersed in a mixture of chloroform/DMF solution containing cisplatin (4.0 mg/mL), followed by the slow evaporation of the solvents under a nitrogen gas. During this solvent evaporation process, cisplatin was supposed to diffuse into the cavity of the porous hollow NPs through their pores due to the concentration gradient buildup outside the NPs. However, the barrier created by either PEG or original hydrophobic layer prevented cisplatin from entering the void. With all tests performed, the maximum Pt/Fe ratio was less than 5% Pt/Fe wt%) as determined by ICP-AES analysis. To reduce the barrier effect, we carried out the loading by mixing the oleate/oleylamine-coated PHNPs with cisplatin and DPA-PEGs in chloroform/DMF solution followed by solvent evaporation as shown in Figure 2. The idea here is to ensure the presence of cisplatin during the ligand exchange reaction so that the cisplatin diffusion into the void can be maximized. ICP-AES analysis indicated that much higher loading of cisplatin (up to 25%) was indeed obtained.

We investigated the maximum quantity of encapsulated cisplatin in the PHNPs with different pore sizes (Figure S2, Supporting Information). A small amount of cisplatin (~5%) was associated with the nonporous HNPs after its partition into the PEG layer. The amount of cisplatin incorporated in the PHNPs was approximately 5-times of that of the HNPs, indicating that most cisplatin penetrate through the porous shell and enter the hollow voids. The molar ratio of Pt and Cl atoms obtained from EDS was roughly 1:2, consistent with the stoichiometry of Pt and Cl in cisplatin, which proved that the encapsulated cisplatin remained intact during the loading process (Figures S5 and S6, Supporting Information).

Kinetics of Cisplatin Release. To study release kinetics of the encapsulated cisplatin in the Pt-PHNPs-3, we dialyzed the Pt-PHNPs-3 against the PBS buffer at pH 7.4 and 37 °C. The amount of Pt and iron released from the particles was measured by ICP-AES. The cumulative release curves of cisplatin from various Pt-PHNPs were shown in Figure S7 in Supporting Information. The encapsulated cisplatin shows a slow release rate, its $t_{1/2}$ (the time needed for the release of 50% of the dose) is approximately 18 h, comparing to that of free cisplatin at $t_{1/2}$ < 30 min). The release curves fit very well to the semiempirical Korsmeyer−Peppas model that is used to describe the release mechanism.[30] The fitting result obtained from the curve-fitting of Origin (OriginLab) software are presented in Figure S7 in Supporting Information. It indicates that the release of cisplatin is a diffusion-controlled process and follows Fick's law.[30] As the cisplatin predominantly diffuse through the water-filled pores, an expansion of the pore size increases significantly the release rate with their $t_{1/2}$ ranging from 7.4 to 18.8 h (Figure S7, Supporting Information). Therefore, the pore size control can be used to optimize cisplatin release rate.

(28) (a) Xu, C.; Wang, B.; Sun, S. *J. Am. Chem. Soc.* **2009**, *131* (12), 4216. (b) Wang, B.; Xu, C.; Xie, J.; Yang, Z.; Sun, S. *J. Am. Chem. Soc.* **2008**, *130* (44), 14436.

(29) (a) Dhar, S.; Gu, F. X.; Langer, R.; Farokhzad, O. C.; Lippard, S. J. *Proc. Natl. Acad. Sci. U.S.A.* **2008**, *105*, 17356. (b) Ajima, K.; Yudasaka, M.; Maigne, A.; Miyawaki, J; Iijima, S. *J. Phys. Chem. B* **2006**, *110*, 5773. (c) Ajima, K.; Maigne, A.; Yudasaka, M.; Iijima, S. *J. Phys. Chem. B* **2006**, *110*, 19097.

(30) (a) Korsmeyer, R. W.; Lustig, S. R.; Peppas, N. A. *J. Polym. Sci., Part B: Polym. Phys.* **1986**, *24*, 395. (b) Korsmeyer, R. W.; Vonmeerwall, E.; Peppas, N. A. *J. Polym. Sci., Part B: Polym. Phys.* **1986**, *24*, 409. (c) Ritger, P. L.; Peppas, N. A. A. *J. Controlled Release* **1987**, *5*, 23.

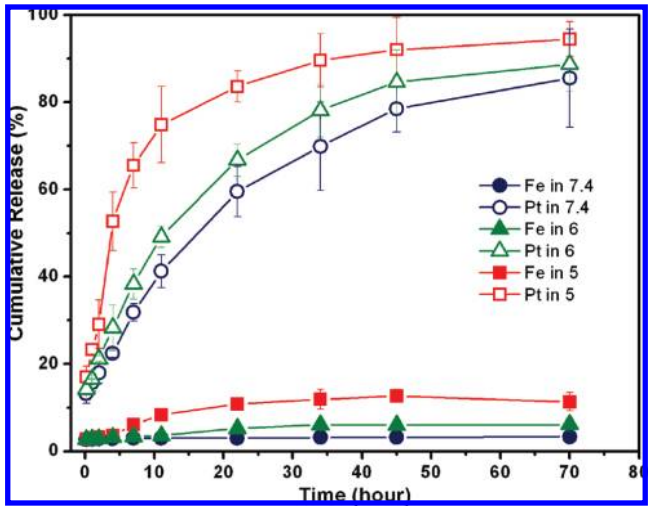

Figure 3. pH-dependent release of cisplatin from Pt-PHNPs (19.6% Pt/Fe). The Pt-PHNPs were incubated in PBS at pH = 7.4 or at pH = 6.0 or 5.0) at 37 °C. In each pH condition, the Pt and Fe released from the PHNPs were measured by ICP-AES.

The release of cisplatin from the Pt-PHNPs was pH-dependent, as shown in Figure 3. Except for the initial burst release, the cumulative release of cisplatin as a diffusion-controlled process under a physiological condition (pH 7.4) shows a gradual increase and reaches a plateau after 48 h with $t_{1/2}$ = 16.4 h. A slow and slightly sustained release rate of the trapped cisplatin in the first 24 h is important for reducing the drug leakage and for protecting cisplatin from inactivation in the physiological environment prior to its reaching the targeting cells.[29] At pH 5.0, the cisplatin release is accelerated with $t_{1/2}$ = 4.0 h. Compared with a negligible change of the iron concentration in the neutral buffer, a concomitant increase in the iron concentration released from Pt-PHNPs at pH 5 after 2 h is also observed, further confirming that the porous Fe_3O_4 shell is subject to the acid etching, resulting in the pore expansion and faster cisplatin release. Considering the pH of the endosomes (pH is near 6) and lysosomes (pH is about 5−6), the Pt-PHNPs offer a desired platform for cisplatin delivery and release.

Target-Specific Delivery of Cisplatin. To develop a cell specific targeting of breast cancer cells, we studied Her-Pt-PHNPs. Herceptin was covalently attached to the amine-reactive groups introduced by activation of the carboxyl groups of the PEG-based cross-linker onto the Pt-PHNP surface using the standard peptide bond-forming methodology (Figure 2). The conjugation was done within 2 h so that the leakage of the encapsulated cisplatin was minimal. To examine whether the conjugated Herceptin was still biologically active, we indentified the ErbB2/Neu expression level of SK-BR-3 cell line by fluorescent immunohistochemical staining using the conjugation of Rhodamine labeled Her-PHNPs. The ErbB2/Neu positivity was recognized by the red fluorescence of SK-BR-3 cell surfaces. As shown in Figures S8 and S9 in Supporting Information, there is no obvious difference in the specific immunofluorescences of the SK-BR-3 cells treated with either Herceptin alone or Her-PHNPs, indicating that the conjugation did not change the Herceptin activity.

The release of cisplatin from the Her-Pt-PHNPs was accelerated by internalization of Her-Pt-PHNPs in the acidic endosomes or lysosomes after cellular uptake. This was believed to involve a receptor-mediated endocytosis pathway. Rab5, as a 24 KDa GTPase that plays an important role in the regulation of the intracellular trafficking and the fusion of endocytic vesicles with early endosomes, is mainly localized to endocytic vesicles and early endosomes and can be used as an early endosome marker.[31,32] After the transfection of a construct (DsRed-Rab5-WT, expressing Rab5 fused with a red fluorescent protein DsRed) to both SK-BR-3 and MDA-MB-231cells, numerous red fluorescent endosomes were observed (Figure 4, DsRed column or Figures S10 and S11 in Supporting Information) without obvious effects on the intracellular trafficking. Both SK-BR-3 and MDA-MB-231cells were identified specifically by a DAPI nucleic acid dye (pseudocolored blue). The cellular uptake and internalization of the FITC labeled Her-Pt-PHNPs were visualized as green fluorescent dots inside the cells (Figure 4, FITC column or Figure S10 and S11, Supporting Information). It can be seen that a significant amount of green fluorescent Her-Pt-PHNPs are internalized in SK-BR-3 cells, but only a few such NPs are taken by MDA-MB-231cells. This is attributed to the fact that ErbB2/Neu overexpression level of SK-BR-3 cell is much higher than that of MDA-MB-231cells.

To examine whether the Her-Pt-PHNPs were localized in the endosomes of SK-BR-3 cells after cellular uptake, the colocalization of Her-Pt-PHNPs and a red-fluorescence-tagged Rab5 was studied. Almost all of Her-Pt-PHNPs were found colocalized in the endosomal compartment with most of the early endosome marker Rab5, as evidenced by the appearance of the yellow color after the overlay of three channels. It suggests that the cellular uptake of Her-Pt-PHNPs undergoes receptor-mediated endocytosis. However, no significant colocalization of Her-Pt-PHNPs and endosomes was detected in MDA-MB-231cells, as a result of the absence of ErbB2/Neu on the plasma membrane. The result from the confocal images of the colocalization of Her-Pt-PHNPs and endosomes was further confirmed by TEM analysis on the internalization of Her-Pt-PHNPs in SK-BR-3 cells. As seen in Figure 5, numerous Her-Pt-PHNPs are found to be attached to the membrane wall of the newly formed endocytic vesicle instead of in the center of the vesicle, confirming that Her-Pt-PHNPs are sufficiently internalized by a receptor-mediated endocytosis, and end up in the acidic endosomes and lysosomes.

In Vitro Cytotoxicity of Her-Pt-PHNPs. As discussed previously, the Her-Pt-PHNPs exhibit slow release of cisplatin in neutral physiological condition but this release is accelerated in endosomal/lysosomal environments. Therefore, with their targeting capability, Her-Pt-PHNPs can introduce high/selective toxicity to the breast cancer cells. The in vitro cytotoxicities of Pt-PHNPs and Her-Pt-PHNPs on SK-BR-3 cells are presented in Figure 6. Both Pt-PHNPs and Her-Pt-PHNPs demonstrate a dose-dependent cytotoxic effect in SK-BR-3 cells, which is slightly lower than that observed with an equivalent dose of free cisplatin after 24 h of incubation. This is probably because the NPs internalized into the cells via the endocytosis are first sequestrated in the endosomal compartments instead of the cytoplasm, whereas free cisplatin can passively diffuse through the cell membrane into the cytoplasm and quickly accumulate in the cell nuclei. After 48 h of incubation, however, the Pt-PHNPs, especially Her-Pt-PHNPs, exhibited higher cytotoxicity than free cisplatin. As shown in Figure 6, the IC_{50} of Her-Pt-PHNPs is 2.9 μM, whereas the IC_{50} of free cisplatin is 6.8

(31) Zhang, J.; Schulze, K. L.; Hiesinger, P. R.; Suyama, K.; Wang, S.; Fish, M.; Acar, M.; Hoskins, R. A.; Bellen, H. J.; Scott, M. P. *Genetics* **2007**, *176*, 1307.
(32) Sharma, D. K.; Choudhury, A.; Singh, R. D.; Wheatley, C. L.; Marks, D. L.; Pagano, R. E. *J. Biol. Chem.* **2003**, *278*, 7564.

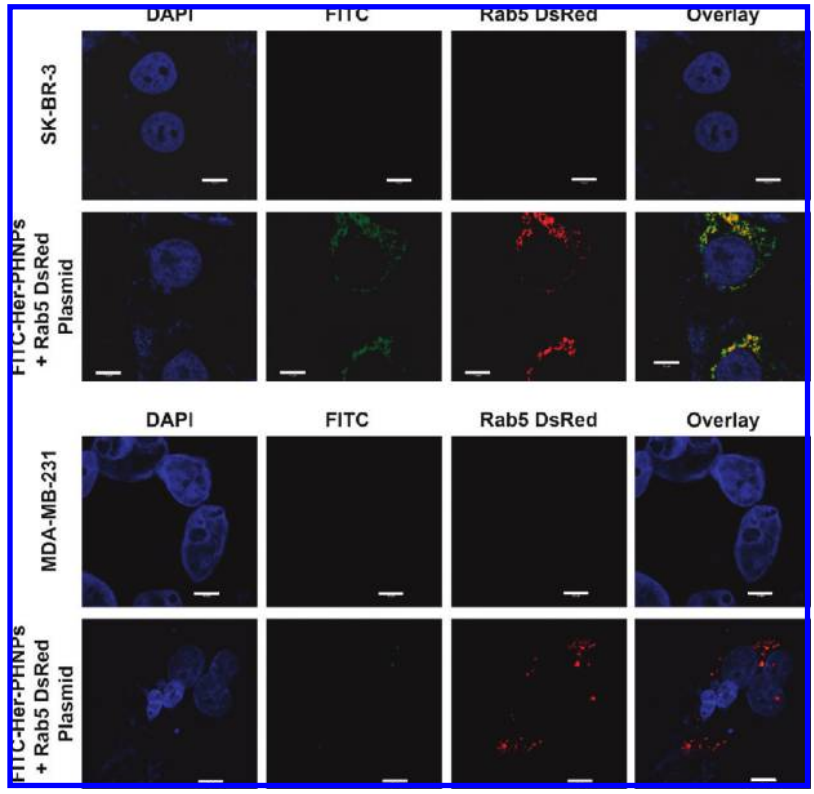

Figure 4. Colocalization of endosome and Her-Pt-PHNPs in SK-BR-3 and MDA-MB-231 cells. Cell monolayers grown on glass coverslips were allowed to near 90% confluence and transfected with Rab5-DsRed WT using Lipofectamine 2000, according to the manufacturer's instructions. FITC-Her-Pt-PHNPs (10 μg Fe/mL in growth medium) were added into the cell culture 10 h after transfection. Control received medium without the particles. After 10 h of incubation, cells were fixed and processed for dual-label immunofluorescence confocal microscopy (CSLM). Cell nuclei are stained with DAPI (pseudocolored blue). Scale bars = 10 μm.

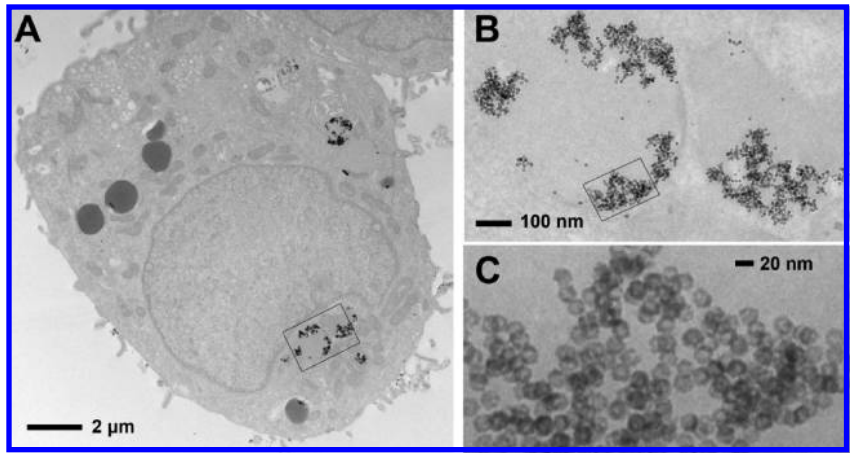

Figure 5. Representative TEM images of a SK-BR-3 cell treated with Her-Pt-PHNPs show the internalization of Her-Pt-PHNPs in the SK-BR-3 cell. After 4 h of incubation, the treated SK-BR-3 cells were fixed with paraformaldehyde, then stained with osmium tetroxide, and subsequently embedded with epoxy−resin. Ultrathin sections were cut with a diamond knife on an Ultracut microtome. (A) Her-Pt-PHNPs are internalized into the SK-BR-3 cell, (B) the internalized Her-Pt-PHNPs trapped inside the endosomes are viewed from an enlarged rectanglar area of (A), (C) the trapped Her-Pt-PHNPs selected from a rectanglar area of (B) show the porous structure.

μM, suggesting that the targeted release and high cytotoxicity of the encapsulated cisplatin in the cells triggered by the endosomal or lysosomal pH.

Conclusions

In summary, we have demonstrated a novel approach using porous hollow NPs (PHNPs) of Fe_3O_4 for targeted delivery and controlled release of the cancer chemotherapeutic drug cisplatin. We constructed the PHNPs to allow their interior cavities to store cisplatin and leave the external surface for biocompatibility and targeting affinity. The release rate of the encapsulated cisplatin from the functionalized Pt-PHNPs could be easily controlled by adjusting the pore sizes and medium pHs. The PHNP structures could not only protect the encapsulated cisplatin from inactivation prior to reaching the target cells but also trigger the fast cisplatin release in low pH endosomes or

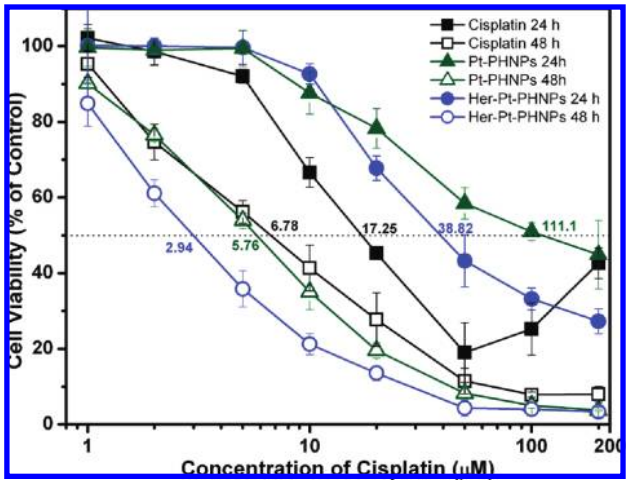

Figure 6. Cytotoxicity of cisplatin (black line), cisplatin-loaded Pt-PHNPs (green line, 19.9% of Pt/Fe), and cisplatin-loaded Herceptin-bound Her-Pt-PHNPs (blue line, 19% of Pt/Fe) to SK-BR-3 cells as a functional of the cisplatin dose after 24 and 48 h of incubation.

lysosomes, resulting in enhanced cytotocixity to these cells. Herceptin-bound PNHPs (Her-Pt-PHNPs) provided an efficient delivery of cisplatin to ErbB2/Neu-positive breast cancer cells (SK-BR-3). The advantages of these PHNPs are that the encapsulated cisplatin within the void is protected from deactivation by plasma protein or other biomolecules prior to reaching the targeted cells, the pH-sensitive pore opening accelerates the cisplatin release in the acidic endosomes/lysosomes once the cisplatin-NPs are internalized to inhibit cell proliferation and to enhance cell apoptosis, and the coupling chemistry reported here is not limited to Herceptin but can be extended to other targeting antibodies or peptides. These advantages, plus the demonstrated superparamagnetic properties of HNPs of Fe_3O_4,[26] indicate that the PHNPs should serve as a contrast enhancement agent for magnetic resonance imaging and as a general platform for target-specific delivery and release of cisplatin for cancer therapy.

Acknowledgment. The work was supported by NIH/NCI 1R21CA12859. We thank Dr. Geoffrey Williams for assistance in obtaining TEM images and Dr. Edward Walsh for useful discussions.

Supporting Information Available: Surfactant synthesis, nanoparticles functionalization, tabulated ICP-AES results, FTIR, XRD, EDS and confocal images. This material is available free of charge via the Internet at http://pubs.acs.org.

JA903300F